

Texture stability of mesoporous ceria made from nanoparticles assembly

L. Yue^{*}, X.M. Zhang

State Key Laboratory of Food Science and Technology, School of Food Science and Technology, Jiangnan University, Wuxi 214122, PR China

Received 19 November 2007; received in revised form 21 December 2007; accepted 4 March 2008

Available online 1 July 2008

Abstract

A supramolecular templating approach to crystalline ceria mesoporous materials had been developed, using inorganic colloidal CeO₂ nanoparticles as building blocks and HF or HCl as binding reagent. Calcination of the supramolecular-templated mesostructures yielded mesoporous ceria materials with high surface areas. The density of the surface hydroxyls was affected by the assembly process adopted as detected by D₂-OH exchange. Structural changes under various treatment conditions were investigated in order to assess the thermal or hydrothermal stability of the obtained materials. The mesoporous ceria with HF as binding reagent exhibited an exceptionally high thermal and hydrothermal stability, which was attributed to the combination of large wall thickness and the surface fluoride ions. The surface F ions prevented the meso-ceria from sintering of nanoparticles.

© 2008 Elsevier Ltd and Techna Group S.r.l. All rights reserved.

Keywords: A. Calcination; B. Nanocomposites; D. CeO₂; Porosity

1. Introduction

Porous materials play important roles in many applications, which stimulate the research interest in developing new synthetic methods for new porous materials, especially for those stable over long periods at high temperatures. Since the hexagonally packed mesoporous silicate materials, i.e., the MCM-41 series with uniform pores and large surface areas surpassing 1000 m²/g, were reported in 1992 [1,2] via a surfactant micelle-assisted process, plenty of research works on porous materials have been documented. The method using surfactant micelles as template has also been used for the preparation of various oxide materials other than silica with high surface area and ordered pore systems [3,4]. Among them, mesoporous transition metal oxides are more widely used as solid catalysts [5,6], catalyst supports [7] and host materials [8] for nanocomposites. Unfortunately, the thermal or hydrothermal stability of these mesoporous materials is in many cases less satisfactory compared with the mesoporous silica. The thin

walls among the pores and re-crystallization of the oxide walls are the reasons for the low thermal or hydrothermal stabilities. Recent progress in this field shows the method of using nanoparticles as the building blocks is a promising strategy to modify the stabilities of mesoporous materials, in which nanoparticles stack to bulk mesostructures [9–15]. Thus materials prepared are viewed important for many applications such as catalysis and high-surface area materials [16].

Cerium oxide has received considerable research attention for its application in various aspects [17–21]. For example, it can be used as active component in combustion catalyst and as an important additive in three-way catalysts for vehicle emission control [22]. And its unique support effect on loaded catalytic metals has been revealed recently [23]. Using the conventional method, meso-ceria has been reported to collapse easily at mild temperatures [24,25]. Corma et al. [12,13] have reported recently the synthesis of the ordered meso-ceria with modified thermal stability via nanoparticle assembly, and they proposed the strong covalent bridges among the nanoparticles by the condensation of surface hydroxyls improve the stability. Deshpande et al. have also reported the evaporation-induced self-assembly of ceria nanoparticles into mesoporous materials [14]. It is noteworthy that the thermal or hydrothermal stabilities of thus prepared meso-ceria have not been addressed

^{*} Corresponding author. Tel.: +86 510 85329059; fax: +86 510 85329081.

E-mail addresses: yuelin@jiangnan.edu.cn (L. Yue),
xmZhang@jiangnan.edu.cn (X.M. Zhang).

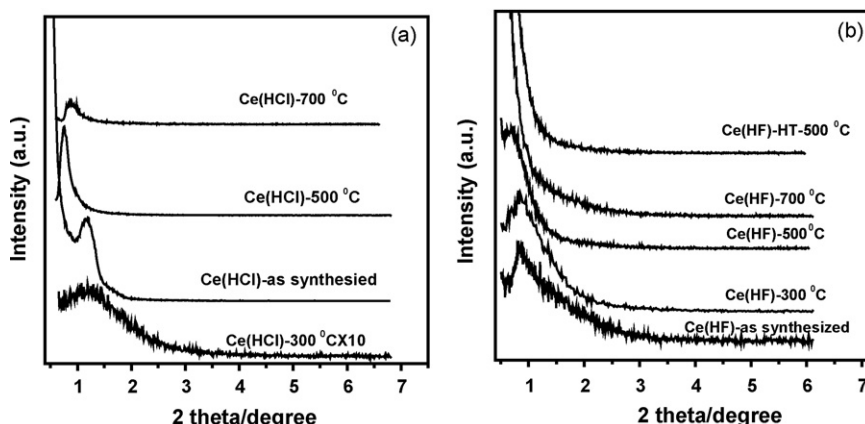


Fig. 1. Small angle X-ray diffraction patterns of mesoporous CeO_2 prepared with (a) HCl (denoted as Ce(HCl)-TTT) and (b) HF (denoted as Ce(HF)-TTT) as binding agent. The TTT means the calcination temperature. Hydrothermally treated samples in 100% steam, are indicated by the characters HT in their names.

well in literature. In this report, we described a new and facile method to synthesize meso-ceria with ~ 5 nm CeO_2 nanoparticles as building blocks, P123 as template and HF or HCl as binding reagent for the combination of nanoparticles with the template. In contrast with the previous studies in the literature, the samples obtained with the present method shows promising thermal and hydrothermal stabilities. The surface fluoride prevents the meso-ceria from sintering.

2. Experimental

2.1. Sample preparation

CeO_2 nanoparticles (~ 5 nm) were obtained using wet chemical process. Gaseous oxygen was bubbled through a gas distributor into a 10 ml $\text{NH}_3\cdot\text{H}_2\text{O}$ (25 wt.%) containing 200 ml distilled water under vigorous stir. 30 mmol $\text{Ce}(\text{NO}_3)_3$ containing 70 ml purified water was pumped continuously into the above aqueous ammonia. The purple precipitate gradually turned to pale yellow with the oxidation of Ce(III) to Ce(IV). The suspension system was continuously stirred overnight at 20°C . The yellow precipitate was then washed with water and recovered by centrifugation. The samples were denoted as Ce-NP in the context.

The assembly of ceria nanoparticles was performed with two procedures. (a) 10 ml of a 0.6 mol L^{-1} CeO_2 sol (~ 1.0 g CeO_2), of which pH was set to 2 by 2 M HCl, was poured into 8 ml aqueous solution of 0.72 g P123 (Pluronic P123 surfactant, MW: 5800, BASF). The mixture was stirred at room temperature for 24 h and followed by aging at 45°C for 48 h without stir. The precipitate was recovered by sedimentation. The sample was denoted as Ce(HCl) in the context. (b) 10 ml of a 0.6 mol L^{-1} CeO_2 sol (~ 1.0 g CeO_2), of which pH was set at 3 by HF, was poured into 0.72 g P123 containing 8 ml water. The resulting suspension was stirred for 24 h at room temperature and allowed to evaporate in a film evaporator. The sample was denoted as Ce(HF) in the context.

All the samples were dried at room temperature and then heated at a rate of $1^\circ\text{C}/\text{min}$ to various temperatures and maintained at that temperature for 6 h in air. The hydrothermal

stability of Ce(HF) sample was performed in a stainless steel reactor. Liquid water (~ 0.1 g/min) was pumped into the preheated zone of the reactor. The steam then travelled through the sample bed. Any carrier gases were not used. The temperature was increased at a rate of $5^\circ\text{C}/\text{min}$ and the Ce(HF) sample was exposed to steam at 500°C or 700°C for 4 h at autogenous pressure with a relative humidity of 100%.

2.2. Sample characterization

The X-ray diffraction patterns of the products were recorded using a Phillip X'pert pro Advance Powder X-ray diffractometer (Cu $\text{K}\alpha$ radiation). Transmission electron microscopy (TEM) micrographs were obtained with a FEI Tecnai G^2 20S-TWIN electron microscopy operating at an acceleration voltage of 200 kV. Nitrogen adsorption/desorption isotherms were recorded using a micromeritics ASAP 2020 instrument. The

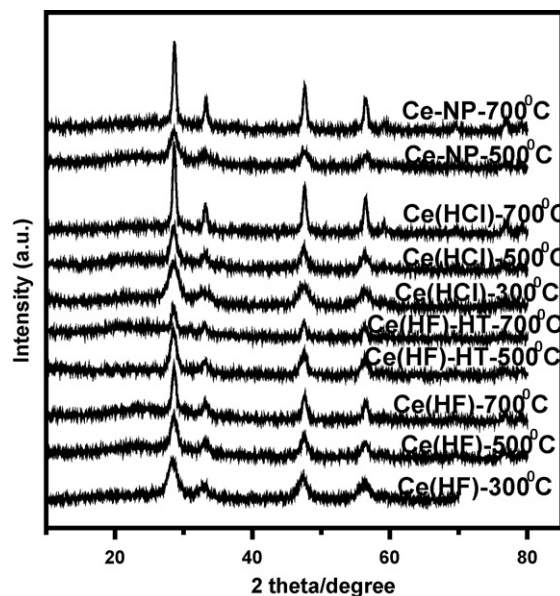


Fig. 2. X-ray powder diffraction patterns of CeO_2 nanoparticles and mesoporous ceria treated at various conditions.

Table 1
The texture properties of samples calcined at different temperatures

Sample	Temperature (°C)	$D_{\text{XRD}}^{\text{a}}$ (nm)	Area (m^2/g)	Pore ^b (nm)	Pore volume (cm^3/g)
Ce-NP-500	500	7.5	88	3.3	0.085
Ce-NP-700	700	16.2	23	3.8	0.037
Ce(HCl)-300	300	5.6	133	3.6	0.108
Ce(HCl)-500	500	9.2	65	3.8	0.091
Ce(HCl)-700	700	16.2	24	3.6	0.034
Ce(HF)-300	300	5.7	126	4.2	0.154
Ce(HF)-500	500	8.5	87	7.3	0.235
Ce(HF)-700	700	12.7	50	6.2	0.112
Ce(HF)-HT-500	500	8.7	84	6.8	0.205
Ce(HF)-HT-700	700	13.3	43	7.6	0.103

^a Ceria crystal size calculated from XRD data using Scherrer equation.

^b Measured by N_2 adsorption.

pore size distribution curves were obtained from the desorption branch calculate by the Barrett–Joyner–Halenda (BJH) method. The density of surface OH groups was measured by D_2 –OH exchange technique. The HD evolution was monitored by mass

spectrometer (Inficon Transceptor 2) at mass to charge ratio of 3. Ar was used as internal standard for calculation. Samples were heated in $100 \text{ cm}^3/\text{min}$ 20% O_2/He at 250°C for 1 hour and cooled down to room temperature in dry helium. Then the

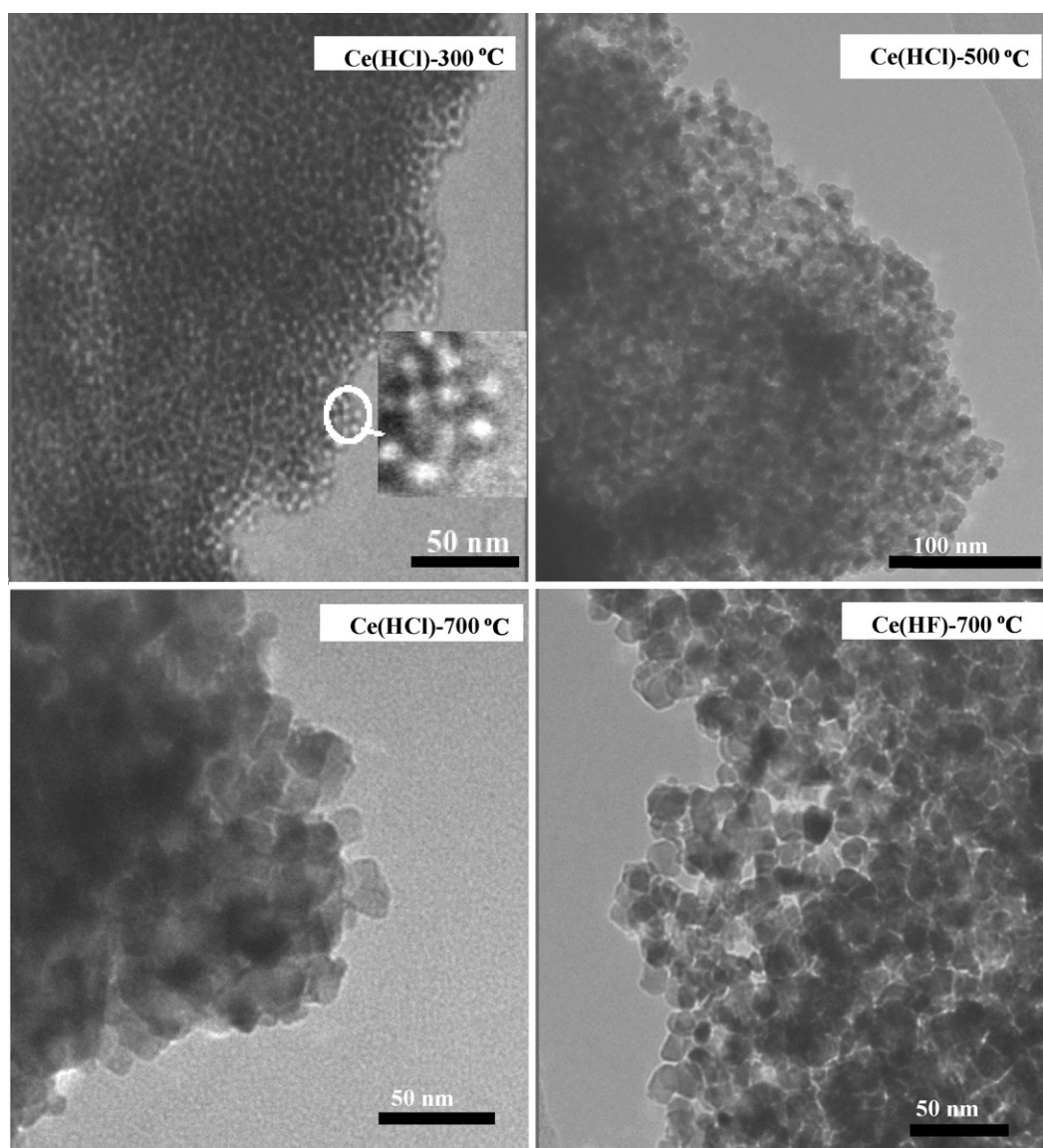


Fig. 3. Typical TEM images of Ce(HCl) and Ce(HF) heated under various temperatures.

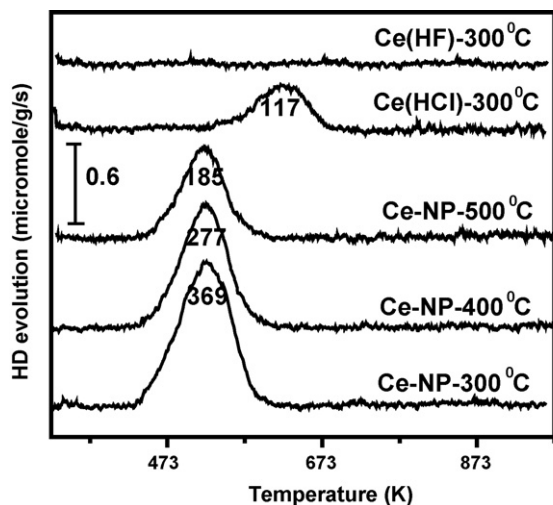


Fig. 4. HD evolution curves during D_2 -OH exchange. The figures in parentheses were the OH density of the samples ($\mu\text{mol/g}$).

flow gases were switched to 5% D_2 /Ar, and the samples were heated at $5^\circ\text{C}/\text{min}$ to perform D_2 /OH exchange.

3. Results and discussion

As shown by XRD results (Fig. 1), all the samples with HCl as binding agent show a first-order reflection around 1° , even

calcined at temperatures as high as 700°C , indicating the mesostructures ordered to some extent. The calcination at high temperatures causes the XRD diffraction peak moves to the lower angle, indicating the growth of nanoparticles, i.e. the pore walls, and increasing in lattice size. But the heat treatment at 700°C causes the XRD peak shrinks and moves to higher angle, implying the partial collapse of ordered porous structures. For the meso-ceria with HF as binding agent, calcination at 500°C or higher temperatures causes the first-order reflection peak to vanish away, implying the breakdown of the ordered mesoporous structure. Likewise, hydrothermal treatment of Ce(HF) in the above mentioned condition also removes the XRD diffraction peaks.

The heat effect on the mesostructures of the materials is complicated. Commonly, a little shift to higher angle of the X-ray diffraction peak by calcination is reasonable. For instance, the Ce(HF) heated at 300°C shows a slight contraction of the mesostructure upon surfactant removal. On the other hand, the heat treatment may shift the X-ray diffraction peaks slightly to lower 2-theta values, due to the growth of nanoparticles during the heat treatment, which should result in a slight enlargement of pores. The finding will be illustrated as follows.

Fig. 2 shows the wide-angle X-ray diffraction patterns of the ceria nanoparticles and the assembled mesoporous samples calcined at various temperatures. All the diffraction peaks can be assigned to cubic fluorite CeO_2 [26]. With increase of the

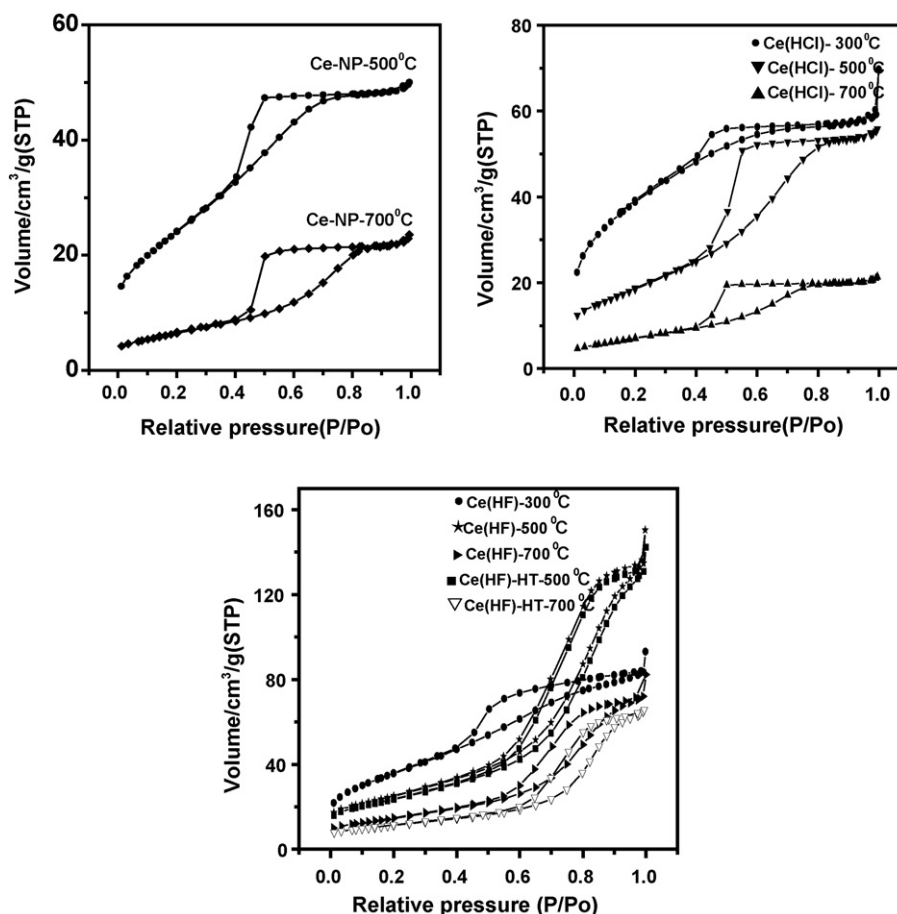


Fig. 5. Nitrogen adsorption-desorption isotherms of the calcined mesostructured ceria and ceria nanoparticles.

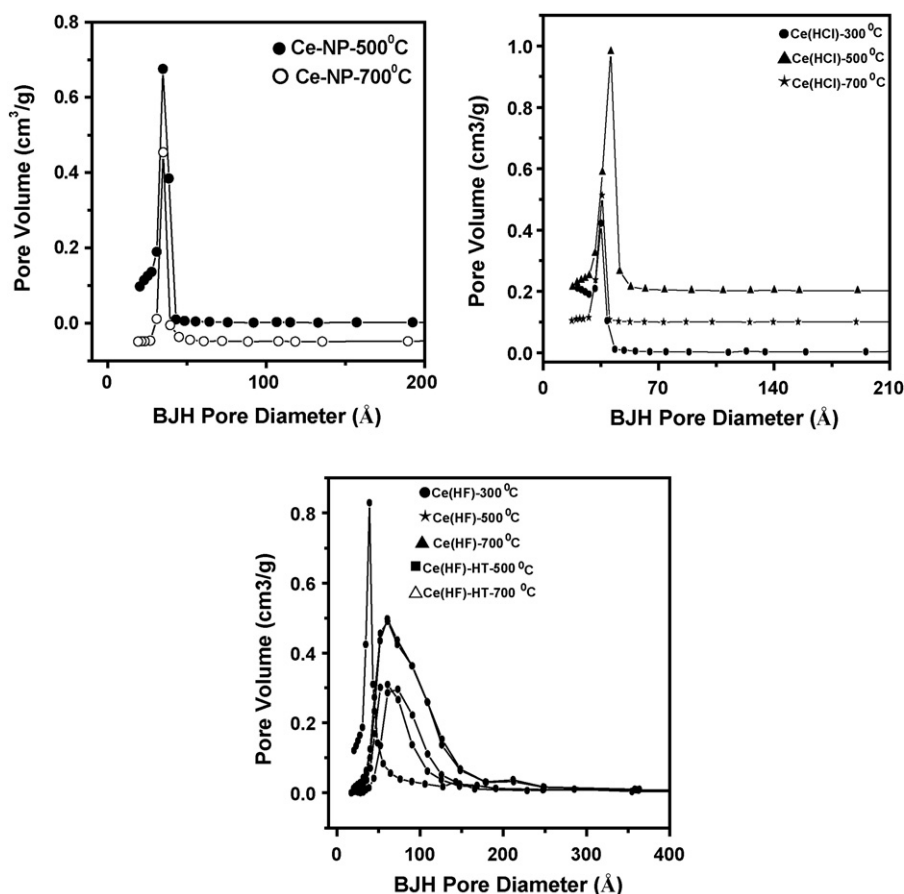


Fig. 6. Pore size distribution of the calcined mesostructure ceria.

calcination temperatures, the peaks become narrower and their intensity increases due to the sintering and agglomeration of ceria crystallites. Crystallite sizes (D_{XRD}) of CeO_2 calcined at various temperatures calculated by Scherrer formula with the width of (1 1 1) diffraction peak are listed in Table 1. The growth of CeO_2 crystallites apparently depends on both the calcination temperature and the methods of assembly. At the same heat temperatures, the size of CeO_2 crystallites for Ce(HF) series is obviously smaller than those of Ce(HCl) series.

The above results are in agreement with the TEM observations, as shown in Fig. 3. The presence of a wormlike mesostructure is apparent, i.e. the mesostructures are not so ordered because there existed only the first XRD diffraction peak. No any additional indexable peak besides the broad d_{100} peak is observed. At the respective temperature of 300 °C and 500 °C, TEM images of Ce(HCl) and Ce(HF) exhibit the great similarity, whereas at the temperature of 700 °C, their TEM images show a significant difference. The TEM of the samples heated at 500 °C shows the presence of dense wormlike mesopores due to the sintering and the growth of the nanoparticles. For the samples heated at 700 °C, their TEM photos show a rather foamlike structure made of closely packed nanoparticles. The nanoparticles in Ce(HCl) or Ce-NP heated at 700 °C pack more closely than those of Ce(HF).

In the current strategy for assembly, the surface functionalization by F^- or Cl^- ions is important. The halides are possible to substitute the surface hydroxyl groups and then to influence the property of thermal stability and hydrothermal stability of the materials at the end. The density of surface hydroxyls of Ce-NP and assembled mesoporous ceria is detected by the technique of D_2 -OH exchange [27–29]. Fig. 4 shows the HD evolution curves during D_2 -OH exchange. For Ce-NP calcined at 300 °C, 400 °C and 500 °C, the maximum rate of HD evolution is observed at the same temperature (250 °C), but the hydroxyl density decreases with the increase of calcination temperature. In contrast the surface hydroxyls for assembled mesoporous ceria are different from nanoparticles. For Ce(HCl), the HD evolution peak centers at around 370 °C, about 120 °C higher than that of ceria nanoparticles, indicating the chlorides remove the sites for D_2 dissociation on the surface of mesoporous ceria. Compared with ceria nanoparticles, only 35% hydroxyls are reserved after assembly. It is noteworthy that no hydroxyls are detected for Ce(HF), indicating that the fluoride replaced all the surface hydroxyls of ceria during assembly with HF as binding agent. Accordingly, fluorides in great amount are detected by chemical analysis of Ce(HF), equal to the surface OH density of ceria nanoparticles.

The results of D_2 -OH exchange reveal the decrease in surface OH groups after assembly, indicating the substitution of

surface OH groups by halide F or Cl ions. Moreover, the F ions are better for surface functionalization because the interaction between the F ions and the protons located at the surface P123 template is stronger than that between Cl ions and protons, the HF is better to bind the ceria colloidal with P123 template. At the same time, F ions, substituting all of the surface hydroxyls, prohibit the condensation among the hydroxyls of ceria, which is the mechanism for sintering of ceria. Higher texture stability can be deduced for Ce(HF) at high temperature in dry air or 100% humidity, compared with Ce(HCl). In addition, Cl ions are easier to leave than F ions, which also reduce strength of repulsion among nanoparticles. These all justify the differences between Ce(HF) and Ce(HCl).

XRD and N₂ adsorption experiments [30] are the most-common methods for assessment of the thermal stability and hydrothermal stability of mesoporous materials. Comparatively, the results of N₂ adsorption are sound to elucidate the texture of the porous materials. Fig. 5 shows the N₂ sorption isotherms of the samples treated under different conditions and Fig. 6 shows the corresponding pore size distribution curves calculated by BJH method from desorption isotherms. Quantitative results are summarized in Table 1. The Ce-NP loses most of its specific surface area, from 88 m²/g at 500 °C to 23 m²/g at 700 °C, but retains the well-defined narrow pore size distribution (Fig. 6). Obviously, the surface area of Ce(HCl) sample decreases more rapidly with the increase of heat temperature, compared with that of the Ce(HF) sample. Under the same thermal treatment conditions, the Ce(HF) shows larger surface area and broader pore size distribution. In agreement with the results of small angle X-ray diffraction, the average pore size of Ce(HF) enlarges when heated at 500 °C, though the nanoparticles grow in size.

Combining the current charactering results, it can be concluded that F[−] on the surface of ceria nanoparticles prevents the meso-ceria from sintering. Even the Ce(HF) is exposed to 100% steam at high temperature of 700 °C when its small angle X-ray diffraction peak removes completely (Fig. 1), its specific surface area and pore size distribution show very little change. The treated Ce(HF) still exhibits a type IV isotherm, indicating the presence of mesoporous structure during the hydrothermal treatment (Fig. 5).

There is a very interesting phenomenon that should be stated here. The pore size and pore volume of Ce(HF) increase more significantly when it is calcined at 500 °C than when it is at 300 °C.

4. Conclusion

In conclusion, a facile method for synthesis of thermally stable and crystalline mesoporous materials has been developed using ceria nanoparticles as building blocks with HF or HCl as assembling agent to bind the ceria colloidal to the surface of polymer template. The binding agent, i.e., fluoride or chloride, can substitute the surface OH groups of ceria. For the substitution, fluoride is more efficient than chloride, and the mesoporous ceria with HF as binding agent shows higher thermal and hydrothermal stabilities. The presence of surface

fluoride on the surface of ceria nanoparticles is very effective for preventing the meso-ceria from sintering, which then increase the texture stability of ceria.

Acknowledgments

The authors thank the help from Mr. Ding Weiping and Mr. Guo Xuefeng. Without their precious guidance, this article would not be brought out. This work was financially supported by the High Tech Research and Development project of China (2008AA10Z419).

References

- [1] C.T. Kresge, M.E. Leonowicz, W.J. Roth, J.C. Vartulli, J.S. Beck, Ordered mesoporous molecular sieves synthesized by a liquid-crystal template mechanism, *Nature* 359 (1992) 710–712.
- [2] M.E. Davis, Organizing for better synthesis, *Nature* 364 (1993) 391–392.
- [3] J.Y. Ying, C.P. Mehnert, M.S. Wong, Synthesis and applications of supramolecular-templated mesoporous materials, *Angew. Chem. Int. Ed. Engl.* 38 (1999) 56–77, 1999.
- [4] X. He, D.M. Antonelli, Recent advances in synthesis and applications of transition metal containing mesoporous molecular sieves, *Angew. Chem. Int. Ed. Engl.* 41 (2002) 214–229.
- [5] V.F. Stone, R.J. Davis, Synthesis, characterization, and photocatalytic activity of titania and niobia mesoporous molecular sieves, *Chem. Mater.* 10 (1998) 1468–1474.
- [6] D.M. Antonelli, J.Y. Ying, Synthesis of hexagonally packed mesoporous TiO₂ by a modified sol-gel method, *Angew. Chem. Int. Ed. Engl.* 34 (1995) 2014–2017.
- [7] M.P. Kapoor, Y. Ichihashi, K. Kuraoka, W.J. Shen, Y. Matsumura, Catalytic methanol decomposition over palladium deposited on mesoporous cerium oxide, *Catal. Lett.* 88 (2003) 83–87.
- [8] M. Vetrano, M.L. Trudeau, D.M. Antonelli, Synthesis and electronic properties of reduced mesoporous sodium niobium oxides, *Adv. Mater.* 12 (2000) 337–341.
- [9] M.S. Wong, E.S. Jeng, J.Y. Ying, Supramolecular templating of thermally stable crystalline mesoporous metal oxides using nanoparticulate precursors, *Nano Lett.* 1 (2001) 637–642.
- [10] R.K. Rana, L.Z. Zhang, J.C. Yu, Y. Mastai, A. Gedanken, Mesoporous structures from supramolecular assembly of in situ generated ZnS nanoparticles, *Langmuir* 19 (2003) 5904–5911.
- [11] Y. Zhou, D.M. Antonietti, Synthesis of very small TiO₂ nanocrystals in a room-temperature ionic liquid and their self-assembly toward mesoporous spherical aggregates, *J. Am. Chem. Soc.* 125 (2003) 14960–14961.
- [12] A. Corma, P. Atienzar, H. Garcia, J.Y.C. Ching, Hierarchically mesostructured doped CeO₂ with potential for solar-cell use, *Nat. Mater.* 3 (2004) 394–397.
- [13] J.Y.C. Ching, F. Cobo, D. Aubert, H.G. Harvey, M. Airiau, A. Corma, A general method for the synthesis of nanostructured large-surface-area materials through the self-assembly of functionalized nanoparticles, *Chem. Eur. J.* 11 (2005) 979–987.
- [14] S. Deshpande, N. Pinna, B. Smarsly, M. Antonietti, M. Niederberger, Controlled assembly of preformed ceria nanocrystals into highly ordered 3D nanostructures, *Small* 1 (2005) 313–316.
- [15] J.H. Ba, J. Polleux, M. Antonietti, M. Niederberger, Non-aqueous synthesis of tin oxide nanocrystals and their assembly into ordered porous mesostructures, *Adv. Mater.* 17 (2005) 2509–2512.
- [16] D.R. Rolison, Catalytic nanoarchitectures—the importance of nothing and the unimportance of periodicity, *Science* 299 (2003) 1698–1701.
- [17] A. Trovarelli, Catalytic properties of ceria and CeO₂-containing materials, *Catal. Rev. Sci. Eng.* 38 (1996) 439–520.
- [18] M. Flytzani-Stephanopoulos, Nanostructured cerium oxide, *MRS Bull.* 26 (2001) 885–889.

- [19] A. Corma, J.M. López-Nieto, in: K.A. Gschneider, Jr., L. Eyring (Eds.), *Handbook on the Physics and Chemistry of Rare Earths*, vol. 29, Elsevier, Amsterdam, 2000, p. 269 Chapter 185.
- [20] B.C.H. Steele, Appraisal of $\text{Ce}_{1-y}\text{Gd}_y\text{O}_{2-y/2}$ electrolytes for IT-SOFC operation at 500 degrees C, *Solid State Ionics* 129 (2000) 95–110.
- [21] E.P. Murray, T. Tsai, S.A. Barnett, A direct-methane fuel cell with a ceria-based anode, *Nature* 400 (1999) 649–651.
- [22] A.J. Zarur, J.Y. Ying, Reverse microemulsion synthesis of nanostructured complex oxides for catalytic combustion, *Nature* 403 (2000) 65–67.
- [23] J. Guzman, S. Carrettin, J.C. Fierro-Gonzalez, Y.L. Hao, B.C. Gates, A. Corma, CO oxidation catalyzed by supported gold: cooperation between gold and nanocrystalline rare-earth supports forms reactive surface superoxide and peroxide species, *Angew. Chem. Int. Ed. Engl.* 44 (2005) 4778–4781.
- [24] D. Terribile, A. Trovarelli, J. Llorca, D. Leitenburg, G. Carla, Dolcetti, The synthesis and characterization of mesoporous high-surface area ceria prepared using a hybrid organic/inorganic route, *J. Catal.* 178 (1998) 299–308.
- [25] D.M. Lyons, K.M. Ryan, M. Morris, Preparation of ordered mesoporous ceria with enhanced thermal stability, *J. Mater. Chem.* 12 (2002) 1207–1212.
- [26] JCPDS card number 43-1002.
- [27] W.P. Ding, S.Z. Li, G.D. Meitzner, E. Iglesia, Methane conversion to aromatics on Mo/H-ZSM5: structure of molybdenum species in working catalysts, *J. Phys. Chem. B* 105 (2001) 506–513.
- [28] D. Martin, D. Duprez, Mobility of surface species on oxides. 2. Isotopic exchange of D_2 with H of SiO_2 , Al_2O_3 , ZrO_2 , MgO , and CeO_2 : activation by rhodium and effect of chlorine, *J. Phys. Chem. B* 101 (1997) 4428–4436.
- [29] C. Thomas, L. Vivier, A. Travert, F. Maugé, S. Kasztelan, G. Pérot, Deuterium tracer studies on hydrotreating catalysts. 2. Contribution of the hydrogen of the alumina support to H–D exchange, *J. Catal.* 179 (1998) 495–502.
- [30] Y. Han, N. Li, L. Zhao, D.F. Li, X.Z. Xu, S. Wu, Y. Di, C. Li, Y. Zou, Y. Yu, F.S. Xiao, Understanding of the high hydrothermal stability of the mesoporous materials prepared by the assembly of triblock copolymer with preformed zeolite precursors in acidic media, *J. Phys. Chem. B* 107 (2003) 7551–7556.